

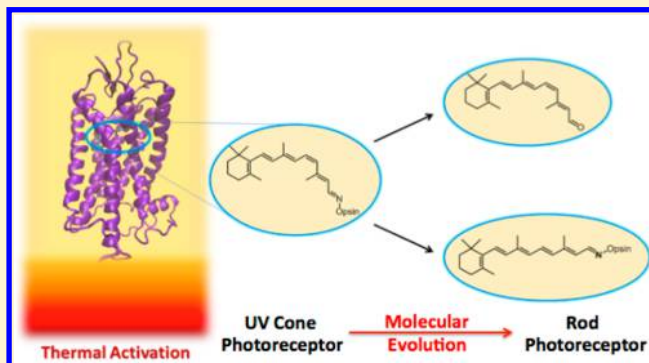
Kinetics of Thermal Activation of an Ultraviolet Cone Pigment

Victoria Mooney,[‡] Sivakumar Sekharan,[‡] Jian Liu,[§] Ying Guo, Victor S. Batista,* and Elsa C. Y. Yan*

Department of Chemistry, Yale University, New Haven, Connecticut 06520 United States

S Supporting Information

ABSTRACT: Visual pigments can be thermally activated via isomerization of the retinyl chromophore and hydrolysis of the Schiff base (SB) through which the retinyl chromophore is bound to the opsin protein. Here, we present the first combined experimental and theoretical study of the thermal activation of a Siberian hamster ultraviolet (SHUV) pigment. We measured the rates of thermal isomerization and hydrolysis in the SHUV pigment and bovine rhodopsin. We found that these rates were significantly faster in the UV pigment than in rhodopsin due to the difference in the structural and electrostatic effects surrounding the unprotonated Schiff base (USB) retinyl chromophore in the UV pigment. Theoretical (DFT-QM/MM) calculations of the *cis*–*trans* thermal isomerization revealed a barrier of ~23 kcal/mol for the USB retinyl chromophore in SHUV compared to ~40 kcal/mol for protonated Schiff base (PSB) chromophore in rhodopsin. The lower barrier for thermal isomerization in the SHUV pigment is attributed to the (i) lessening of the steric restraints near the β -ionone ring and SB ends of the chromophore, (ii) displacement of the transmembrane helix 6 (TM6) away from the binding pocket toward TMS due to absence of the salt bridge between the USB and the protonated E113 residue, and (iii) change in orientation of the hydrogen-bonding networks (HBNs) in the extracellular loop 2 (EII). The results in comparing thermal stability of UV cone pigment and rhodopsin provide insight into molecular evolution of vertebrate visual pigments in achieving low discrete dark noise and high photosensitivity in rod pigments for dim-light vision.



INTRODUCTION

Two types of photoreceptor cells are expressed in vertebrate retina: rods and cones.^{1–4} Rod cells express rhodopsin as a visual pigment for dim-light vision, while cone cells express cone visual pigments for color vision. Both rhodopsin and cone visual pigments are molecular light detectors, belonging to G protein-coupled receptors that share a 7-helical transmembrane protein structure. Their protein is linked to a vitamin A derivative, the 11-*cis* retinal chromophore, through a Schiff base (SB).⁵ The chromophore absorbs a photon and undergoes 11-*cis* to all-*trans* isomerization leading to the formation of Metarhodopsin II (Meta II), which is the active G protein-binding intermediate of rhodopsin in which the retinal SB is still intact but deprotonated.⁵ Finally, the all-*trans* retinal leaves the visual pigment by breaking the covalent SB linkage and enters the retinal pigment epithelium to convert back to 11-*cis* retinal.^{4,6–9}

In the molecular evolution of vertebrate vision, cone pigments first diverged for color vision before evolving to rod pigments (rhodopsin) for dim-light vision.^{1,3,10} The cone pigments belong to four classes: middle and long wavelength-sensitive (M/LWS) pigments, short wavelength-sensitive type 2 (SWS2) pigments, short wavelength-sensitive type 1 (SWS1) pigments, and rhodopsin-like (RH2) pigment.^{11–16} As these pigments evolved from M/LWS to RH1, rhodopsin attained increased photosensitivity for dim-light vision.

There are three main characteristics that enhance the sensitivity of a photoreceptor cell: high signal amplification, high quantum yield, and low dark-noise. When applying these concepts to visual pigments, quantum yield and dark-noise are the only properties that are directly influenced by the structure and function of the photoreceptors. Dark noise, the activation of photoreceptor cells when not caused by absorption of a photon, determines the minimum threshold in vision.^{17–19} The two main sources of photoreceptor noise are discrete dark noise resulting from thermally induced isomerization of 11-*cis*-retinal and continuous dark noise that comes from the constitutive activation of transducin, which can be caused by unbound opsin after hydrolysis of the SB between retinal and opsin. Therefore, these two kinds of dark noise are linked to the two chemical reactions, thermal isomerization and hydrolysis of SB,^{20–23} both of which contribute to the thermal activation of visual pigments.^{24–26} Thermal activation that involves both thermal isomerization and hydrolysis of SB has been previously studied in bovine rhodopsin,^{26,27} but not in cone pigments.

The thermal stability of rhodopsin is aided primarily by steric interactions between the chromophore and the binding pocket and by stabilizing electrostatic and hydrogen-bonding (H-bonding) interactions: an extensive transmembrane hydrogen-

Received: October 14, 2014

Published: December 16, 2014

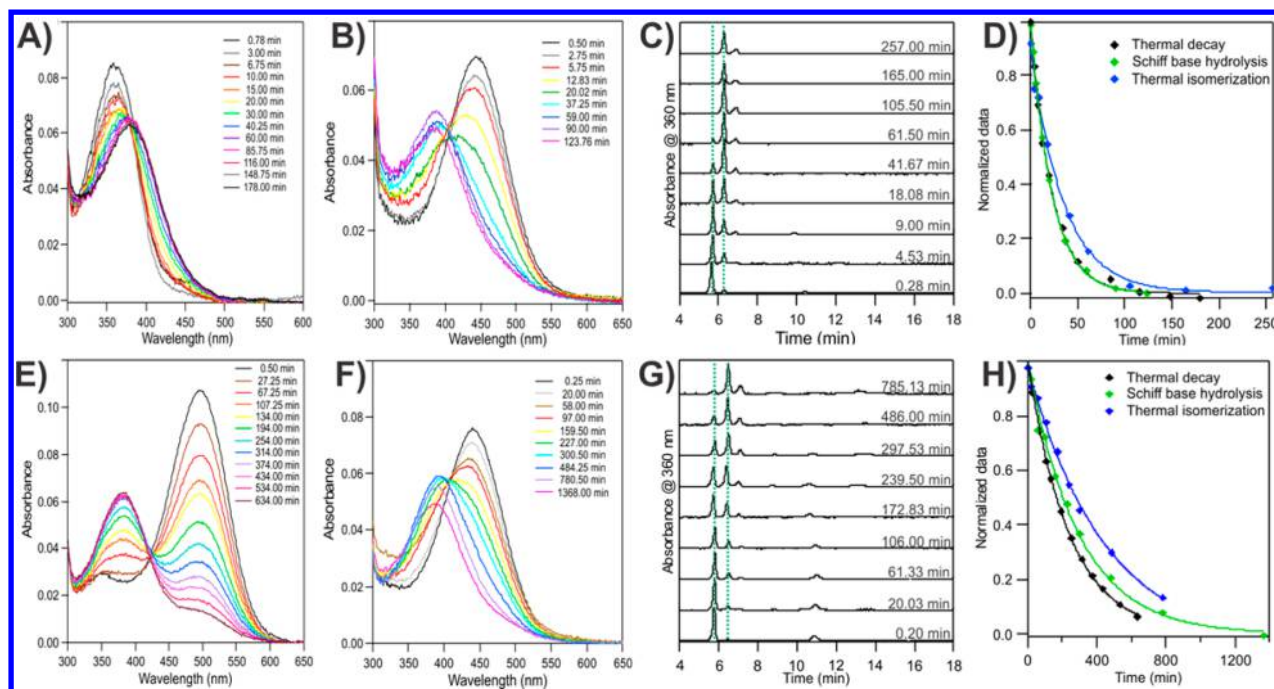


Figure 1. Representative spectra and chromatograms of SHUV thermal stability study. These include data for SHUV (A–D) and Rho (E–H) experiments at 54.7 °C. Data for the thermal decay (A,E), SB hydrolysis (B,F), and thermal isomerization (C,G) experiments are shown as well as their exponential decay fits (D,H). The green dashed lines in the thermal isomerization chromatograms indicate the first and second species to elute, which correspond to the 11-*cis*-15-*syn*-retinaloxime and all-*trans*-15-*syn*-retinaloxime, respectively.

bonding network (HBN) and the ionic interaction between the protonated Schiff base (PSB) and the unprotonated E113 counterion.^{20,28–30} It is not currently known whether cone pigments also have extensive, transmembrane HBNs, but the conservation of the SB's primary counterion, E113 in rhodopsin,³¹ indicates that this residue is universally important for proper photoreceptor function. This has been confirmed across all visual pigment classes, as mutation of this residue causes constitutive activity for all pigment types.³² It has been shown that the E113 residue is also necessary for the proper function of UV pigments, which are unique in that they possess an unprotonated Schiff base (USB).³³ In UV pigments, the E113 residue not only limits constitutive activity³⁴ but also increases the quantum yield of these pigments.^{35,36} However, because the lack of a PSB in UV pigments ensures that the E113 residue can no longer act as a SB counterion in these pigments' dark states, the molecular mechanism by which the E113 residue aids the stability and function of these pigments is not well understood.

The steric and electrostatic differences suggest that the thermal stability of a UV pigment might significantly differ from that of rhodopsin, although to what extent was not previously known. Here, we present the first quantitative study of thermal activations of vertebrate UV cone pigment from Siberian hamster (*Phodopus sungorus*) at ~55 °C and compare the results to those of bovine rhodopsin (Rho). The direct comparison enables us to understand how the thermal isomerization and hydrolysis of SB may have evolved from SWS1 to RH1 pigments. The experimental observations are correlated with the quantum mechanics/molecular mechanics (QM/MM)-based structural models and calculations of the *cis*–*trans* thermal isomerization barrier in SHUV and rhodopsin pigments.

EXPERIMENTAL METHODS

Protein Preparation. A stable cell line of *GnT1*[−] HEK293S cells transfected with the pACMV-TetO vector containing the SHUV gene (GenBank ID: JQ036217) were induced with tetracycline and harvested after 48 h.^{37–39} The proteins were prepared under dim red light, using procedures reported previously.^{37,40–43} The purified UV pigment was suspended Buffer B containing 47 mM HEPES (pH 6.6), 132 mM NaCl, 2.8 mM MgCl₂, 0.02% DM, and 7.5% w/v glycerol during experiments.

Thermal Decay. Experiments were performed as described previously.^{28,29} All experiments took place at 54.7 °C in a UV-2450 Shimadzu spectrophotometer with a variable-temperature cuvette holder connected to a water bath and were performed at least two times for each protein. Approximately 100 μL of concentrated, ice cold, SHUV or Rho pigment was added to 1.0–1.6 mL Buffer B equilibrated at 54.7 °C. UV–vis spectra were collected at various time intervals. The samples were mixed 1–3 times between each aliquot removal during these experiments so that the pigment concentration was identical throughout the sample solution. Since the rate of thermal reactions of visual pigments depends strongly on temperature,^{26,27} 54.7 °C was chosen, such that the rates of thermal reactions of Rho and the UV pigment fell into a time regime (~500 min) that allows kinetic measurements.

Schiff Base Hydrolysis. To determine how stable the dark-state SB linkage is, 100 μL aliquots were removed over the course of a thermal decay experiment and were transferred to eppendorfs containing 7 μL 1 M HCl. These samples were stored on ice until the thermal decay experiment had concluded. UV–vis spectra of these samples were collected after the samples equilibrated at room temperature for ~20 min. The rate of SB hydrolysis in Meta II was determined in a similar way, except that before being added to 54.7 °C Buffer B, the SHUV and Rho pigments were bleached for 2 min on ice. The SHUV pigment was bleached with 365 nm light, and the Rho was bleached using a lamp with a 500 nm long-pass filter.

Retinal Thermal Isomerization. Aliquots of 100 μL were removed during the thermal decay experiments and transferred to glass vials stored on ice. The retinal was extracted in hexane as retinaloxime isomers as previously described.³⁵ The samples were

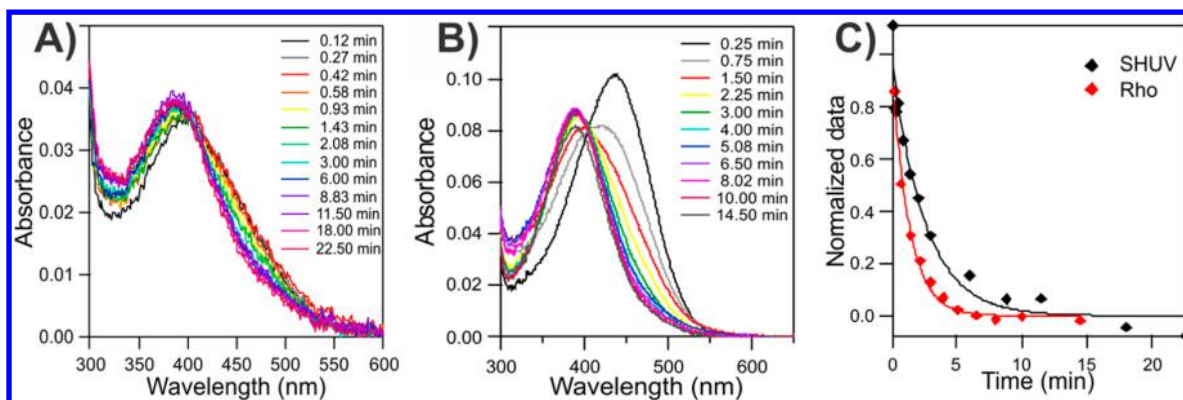


Figure 2. SB hydrolysis during Meta II. Spectra illustrate the decay of SHUV (A) and Rho (B) Meta II states. Data shown were fit to single exponential decays (C).

dried under argon and stored at $-80\text{ }^{\circ}\text{C}$. To determine their isomer composition, the retinaloxime isomers were dissolved in $\sim 25\text{ }\mu\text{L}$ hexane and analyzed via HPLC using a Beckman Coulter SYSTEM GOLD 125 Solvent Module with a silica column (Beckman Coulter Ultrasphere $4.6 \times 250\text{ mm}$). The mobile phase was composed of 8% diethyl ether and 0.33% ethanol in hexane. The Beckman Coulter SYSTEM GOLD 168 Detector measure the absorbance at 360 nm.

RESULTS AND DISCUSSION

Many UV-vis absorption spectra were collected during the SHUV and Rho thermal decay experiments (Figure 1A,E). All of the UV-vis spectra for both the thermal decay and hydrolysis experiments were normalized to the 280 nm protein peak. This was done in order to negate any change in the intensity of the pigments' maximum absorption wavelengths (λ_{max}) caused by a change in pigment concentration resulting from solvent evaporation. Each spectrum collected during the thermal decay experiments was fit to three Gaussian functions.

One Gaussian peak was centered at $\sim 280\text{ nm}$ and is due primarily to the aromatic amino acids present in the proteins. An additional Gaussian peak was centered at the λ_{max} of either dark-state SHUV (359 nm) or dark-state Rho (498 nm). The final Gaussian function used to fit the SHUV and Rho spectra was centered at $\sim 380\text{ nm}$ and was due to retinal in the all-*trans* form and/or with a hydrolyzed SB. As the thermal decay experiments progressed, the dark-state SHUV and Rho pigments underwent thermal activation, which is seen spectroscopically as the pigments' λ_{max} peak decreased and the 380 nm peak grew in (Figure 1A,E).

The spectra collected for the SB hydrolysis of the dark-state pigments (Figure 1B,E) were also fit to three peaks at ~ 280 , 440, and 380 nm. The 440 nm peak is due to an intact SB linkage between retinal and a denatured pigment, while the 380 nm peak is from free retinal. As the experiments progress, the retinal SBs hydrolyzes, and the peak due to the intact SB (440 nm) decreases, while the free retinal peak (380 nm) grows in. In addition, the last samples collected during these experiments do not appear to go through the isobestic point of the previous spectra. This could be due to thermal isomerization of free 11-*cis* retinal to all-*trans* retinal or due to a change in the scattering background due to possible protein aggregation at the later stages of the incubation. However, the last few spectra do not affect the calculation of the decay rates because the 440 nm peaks, the intensities of which are used to determine the decay rates, have almost entirely disappeared in these spectra.

The thermal isomerization chromatograms (Figure 1C,G) were fit to 6 peaks from 11-*cis*-15-*syn*-, all-*trans*-15-*syn*-, 13-*cis*-

15-*syn*-, 13-*cis*-15-*anti*-, 11-*cis*-15-*anti*-, and all-*trans*-15-*anti*-retinaloximes, with the 15-*anti*-isomers being much broader and less intense.^{26,35} The 15-*syn*/15-*anti*-retinaloxime pairs occur during the formation of the retinaloxime, but each pair originates from the combined bound and unbound forms of each of the 11-*cis*, all-*trans*, and 13-*cis*-retinal isomers. The first three species to elute are 11-*cis*-15-*syn*-, all-*trans*-15-*syn*-, and 13-*cis*-15-*syn*-retinaloxime. As the pigments undergo thermal decay, the amount of 11-*cis* retinal is seen in the decrease in 11-*cis*-15-*syn*-retinaloxime and the increase in all-*trans*-15-*syn*-retinaloxime (Figure 1C,G, peaks marked with green, dashed lines), with the 13-*cis*-15-*syn*-retinaloxime peak increasing as well. Once the peak areas were normalized according to their extinction coefficients, the peak areas of each 15-*syn*/15-*anti* pair were combined.

The contribution of 11-*cis* retinaloxime to the overall retinaloxime isomer composition was calculated and subsequently the total amount of 11-*cis* retinal present in the sample.

In addition to data collected during the thermal decay of dark-state Rho and SHUV, spectra revealing the hydrolysis of the SB between all-*trans* retinal and the pigments in their Meta II states were also collected. These spectra were fit in the same manner as those collected during the SB hydrolysis of the dark state (Figure 2). Again, there is a decrease in the 440 nm peak and an increase in the 380 nm peak intensity as the SB hydrolyzes in the activated pigment. The average thermal decay rates determined for wild-type SHUV pigment and rhodopsin from 4 to 9 data sets each were found to be $25 \pm 1\text{ min}$ and $272 \pm 1\text{ min}$, respectively. While it is possible to directly fit the dark-state SB hydrolysis and thermal isomerization data to single exponential decay curves, these decay rates would not take into account the complexity of the entire thermal decay mechanism (Figure 3), as discussed in our previous study.²⁶ Thus, rather than fitting each set of data individually, a global fitting routine based on the model presented for rhodopsin in Liu et al. 2011 and the Meta II hydrolysis rates of the pigments allowed for the simultaneous fitting of the thermal decay, thermal isomerization, and hydrolysis data. Since thermal isomerization and hydrolysis of SB are competing with each other, we investigated two competing pathways of thermal reactions where (i) thermal isomerization precedes hydrolysis of SB and (ii) hydrolysis of SB precedes thermal isomerization.

Using the independently measured Meta II hydrolysis data to determine the decay times of hydrolysis of all-*trans* retinal ($\tau_{\text{hyd}}^{\dagger}$), the normalized data from the other three experiments,

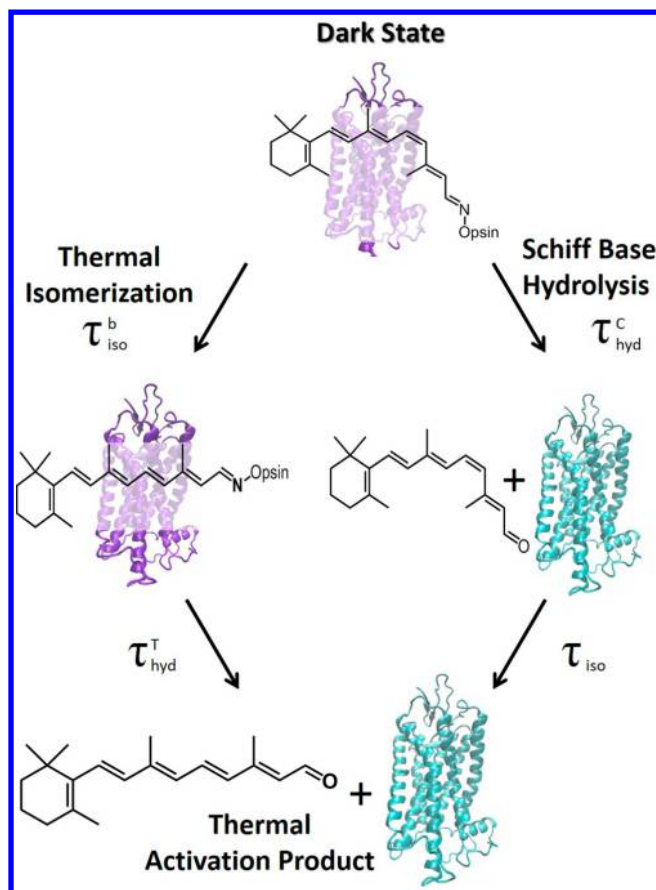


Figure 3. Thermal activation of vertebrate UV visual pigments. Thermal isomerization ($\tau_{\text{iso}}^{\text{b}}$) and SB hydrolysis ($\tau_{\text{hyd}}^{\text{c}}$) cause the formation of two intermediate states. These two intermediates then decay to form a common product upon hydrolysis of the bound all-*trans* retinal ($\tau_{\text{hyd}}^{\text{c}}$) or isomerization of the free 11-*cis* retinal (τ_{iso}). Visual pigments with bound retinal are shown in purple, while opsin is in cyan. The mechanisms shown are based on previously published work.²⁶

and the global fitting strategy previously described,²⁶ the decay times for the SB hydrolysis of 11-*cis* retinal ($\tau_{\text{hyd}}^{\text{c}}$) and the 11-*cis* to all-*trans* isomerization of bound retinal ($\tau_{\text{iso}}^{\text{b}}$) and free retinal (τ_{iso}) were determined (Table 1).

Once the parameters were obtained from the global fitting, the relative contributions of the thermal isomerization and SB hydrolysis to the thermal decay of the SHUV and Rho pigments were determined (Table 1). The results show that the rates of both thermal isomerization and hydrolysis are significantly faster in SHUV than in rhodopsin.

Typically, cone pigments produce more dark noise^{44–46} and have faster Meta II decay rates^{47,48} when compared to rhodopsin rod pigments. Here, the rates of Meta II SB hydrolysis for the SHUV and Rho visual pigments seem to have

deviated from this trend. Previous studies show that there are several opsin characteristics that can influence the rate of SB hydrolysis in Meta II. These include solvent accessibility and the E113 electrostatic interactions,⁴⁹ the surrounding HBN,²⁰ and residues 122 and 189.^{48,50} E113 is conserved in SHUV, and residues L122 and P189, which are common in cone pigments, have not mutated to the residues found in rhodopsin, E122 and I189, which are responsible for the pigment's decreased rate of Meta II decay.^{48,50} This indicates that E113, L122, and P189 are not responsible for the slowed rate of Meta II decay when compared to that of rhodopsin. This suggests that, compared to other cone pigments, there is either a significant change in the SHUV Meta II HBN or the binding pocket has become less solvent accessible, thus hindering access of external water molecules to the binding pocket and preventing SB hydrolysis.⁵¹ Further investigation is necessary to determine which of these two photoreceptor characteristics causes the decrease in the rate of Meta II SB hydrolysis in SHUV.

While the SHUV pigment does not exhibit typical cone pigment behavior with regards to Meta II SB hydrolysis, the decreased thermal stability of cone pigments is reinforced here for the SHUV pigment. As rhodopsin pigments evolved from ancestral pigments, they acquired various molecular interactions that contribute to the stability of the rod pigments, particularly in the dark state. This increased stability necessitated that these experiments be conducted at 54.7 °C rather than the more physiologically relevant 37 °C. At 37 °C, rhodopsin's thermal decay rates are too slow to be measured within ~24 h, and above 54.7 °C those of SHUV are not too fast for accurate measurement. The SHUV pigment's decreased dark-state stability, when compared to that of bovine rhodopsin, indicates that this pigment lacks some of the critical steric and electrostatic interactions that are responsible for rhodopsin's thermal stability in enhancing photosensitivity for dim-light vision.

The structural arrangement of the rhodopsin binding pocket is known to incorporate many steric interactions between the 11-*cis* retinyl chromophore and the surrounding amino acids. These interactions help contort the chromophore into a twisted conformation,^{52,53} in preparation for rapid photoisomerization. However, they also lock the 11-*cis* retinal chromophore into its dark-state conformation in order to prevent thermal isomerization. Comparison of the QM/MM optimized SHUV and rhodopsin structural models³⁷ shows that the presence of three nonconserved residues, Y191W, I189P, M183L perturbs the arrangement of the EII loop in the UV pigment (Figure 4 A). Absence of the salt-bridge network between the USB and E113 and increase in the number of hydrophobic residues surrounding the β -ionone ring region (Figure 4B,C) offers a likely explanation for the lessening of steric constraints at both ends of the USB chromophore.

The decrease in steric constraints may also be aided by movement of TM6 away from the binding pocket, which, in

Table 1. Decay Times for the Thermal Decay Mechanisms of SHUV and Rho^a

visual pigments	$\tau_{\text{hyd}}^{\text{c}}$ (min)	$\tau_{\text{iso}}^{\text{b}}$ (min)	τ_{iso} (min)	hydrolysis (%)	isomerization (%)
SHUV	2.23 ± 0.12	48 ± 5	17 ± 3	52 ± 4	48 ± 4
Rho	1.65 ± 0.01	653 ± 49	439 ± 62	41 ± 2	59 ± 2

^aThe decay times for Meta II SB hydrolysis ($\tau_{\text{hyd}}^{\text{c}}$), and the values for SB hydrolysis in the dark state ($\tau_{\text{hyd}}^{\text{c}}$), thermal isomerization in the dark state ($\tau_{\text{iso}}^{\text{b}}$), and thermal isomerization of free 11-*cis* retinal (τ_{iso}) were calculated for 54.7°C. The percent contributions of hydrolysis of 11-*cis* and isomerization of bound 11-*cis* to thermal decay are also shown.

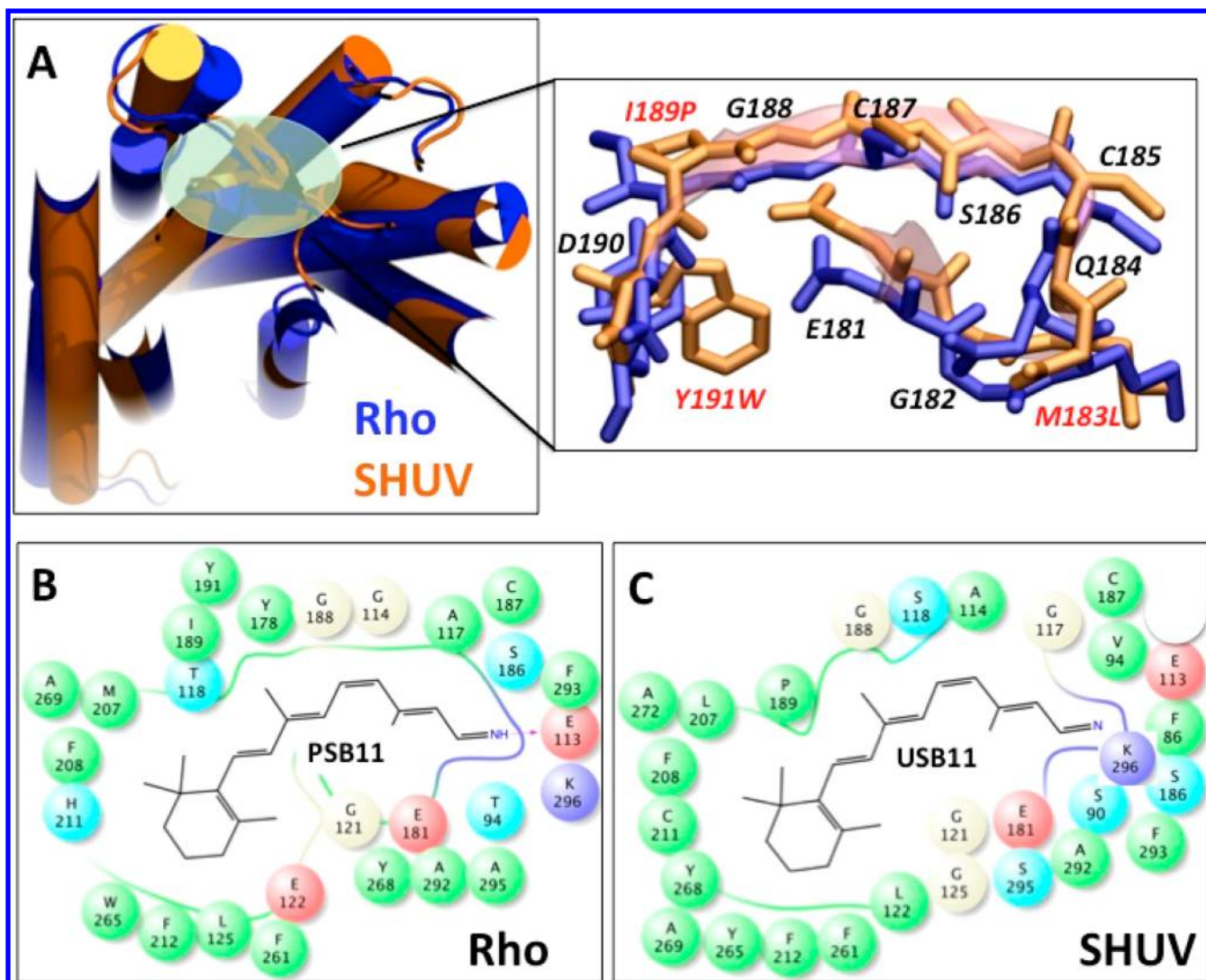


Figure 4. Overlay of the QM/MM optimized structures of bovine rhodopsin and SHUV pigment. (A) The EII loops of bovine rhodopsin (blue) and SHUV (orange) are overlaid to show the displacement of SHUV's loop due to the three nonconserved residues (labels in red show the rhodopsin-to-SHUV mutations). The ligand–protein interaction diagram reveals several polar (blue), hydrophobic (green), and charged (negative (red); positive (blue)) residues lining the chromophore binding pocket of bovine rhodopsin (B) and SHUV (C) pigments. Presence of a strong electrostatic interaction via a hydrogen bond (magenta dashed lines) between protonated SB of 11-*cis* retinyl chromophore (PSB11) and E113 counterion residue in rhodopsin (B) is also shown.

turn, leads to a significant increase in the pigment's dark noise. In fact, Khorana and co-workers found that the salt bridge between E113 and the PSB is necessary to hold TM6 in the dark-state conformation in rhodopsin.⁵⁴ The lack of this crucial salt bridge network in SHUV may allow TM6 to shift toward TM5 making the dark-state conformation similar to the rhodopsin's active state, leading to increased thermal activation. In fact, the average RMSD per residue is 1.3 Å for TM6 residues in the QM/MM model (Figure S3 and Table S2).

HBNs have been proposed to contribute greatly to the thermal stability of visual pigments.^{29,55,56} The SHUV pigment possesses several mutations, G90S, Y191W, and W265Y, which alter its HBN within the binding pocket.³⁷ In the presence of USB in SHUV, the neutral (protonated) form of E113 is stabilized as a H-bond donor to S186, which in turn, becomes a H-bond donor to E181 in the EII loop (Figure S2). Therefore, protonation state of SB can alter the orientation of the HBNs in the retinal binding site, which may affect both thermal isomerization and SB hydrolysis.

To determine the effect of structural differences on thermal isomerization, we performed QM/MM calculations of *cis*–*trans* isomerization in the SHUV pigment. Relaxed intermediate structures along the isomerization minimum energy path are obtained subject to constraint of incremental changes of the C₁₁=C₁₂ dihedral angle ($\phi_{C_{11}=C_{12}}$) from *cis* (−18°) to *trans* (−180°), relaxing the configuration of residues and waters within a 4 Å radius from any atom of the retinyl chromophore (for details see Table S1). We find that the *cis*–*trans* isomerization barrier is significantly lower in the SHUV pigment (~23 kcal/mol) compared to rhodopsin (~40 kcal/mol).²² The QM/MM calculated values are also in excellent agreement with the calculated values of ~23 and ~45 kcal/mol obtained by Barlow et al.,⁵⁷ using the MNDO/AM1 and INDO/PSDCI molecular orbital theory methods. We attribute the decrease in the isomerization barrier in the SHUV pigment to, the change in the protonation state of the SB, lessening of the steric constraints in the binding pocket, displacement of the TM6 due to absence of the salt-bridge between USB and

protonated E113, and change in the orientation of the HBNs in the active site. Additional factors, such as the proposed NPxxY gate,⁵⁹ have been suggested to affect the thermal properties of visual pigments.

While the E113 residue continues to play an active role in rearranging the SHUV HBNs and to the pigment's activation mechanism,⁵⁸ it no longer contributes to the stability of the SB by acting as a PSB counterion in the dark state. In rhodopsin, this salt bridge is important to the pigment's thermal stability. Janz and Farrens showed that the rhodopsin E113Q mutant's thermal stability decreases greatly compared to wild-type and that the rate is also pH dependent. When this mutant's SB is deprotonated at higher pHs, there is another significant increase in the rate of hydrolysis.²¹ This suggests that it is not only the loss of the E113/PSB salt bridge that destabilized the SB, but also the protonation state of the SB that affects that hydrolysis rate. Thus, our data seem to offer indirect support to the thermal activation mechanism proposed by Barlow et al.,⁵⁷ who suggested that rhodopsin's thermal activation occurs during a transient conformation involving USB. The presence of an USB in SHUV, unless counteracted by another stabilizing mechanism, results in a significant decrease in the stability of the dark-state SB linkage.

CONCLUSION

Our combined experimental and computational investigation into the thermal activation of the Siberian hamster UV pigment revealed, for the first time, the relative contributions of thermal isomerization and SB hydrolysis to cone pigment dark noise, which, at ~55 °C, are approximately equal. We also found that the thermal stability of SHUV is significantly less than that of bovine rhodopsin due to an increase in the rates of thermal isomerization and SB hydrolysis. Computational analysis of the SHUV model suggests that there are likely several structural and electrostatic interactions that differ from those in rhodopsin, which contribute to SHUV's decreased thermal stability.

The most significant contribution to decreased thermal stability of the SHUV pigment is the change in protonation state of the SB, which, in turn, changes the orientation of the HBNs in the active site. The thermal isomerization is influenced by a decrease in the steric restraints at both ends of the chromophore leading to lower *cis*–*trans* isomerization barrier. Therefore, we suggest that the molecular interactions, which minimize thermal isomerization and SB hydrolysis in rhodopsin, thus allowing increases photosensitivity and dim-light vision, developed subsequent to the evolution of UV pigments.

ASSOCIATED CONTENT

Supporting Information

Comparison of the HBNs in the SHUV and rhodopsin models. This material is available free of charge via the Internet at <http://pubs.acs.org>.

AUTHOR INFORMATION

Corresponding Authors

victor.batista@yale.edu

elsa.yan@yale.edu

Present Address

[§]Department of Chemistry, Boston University, Boston, MA 02215, United States

Author Contributions

[‡]These authors contributed equally.

Notes

No competing financial interests have been declared.

The authors declare no competing financial interest.

ACKNOWLEDGMENTS

The authors thank the National Eye Institute (NEI) for providing 11-*cis* retinal and NERSC for supercomputer time. This work was funded by the NSF fellowship DGE-0644492 awarded to V.L.M., NSF Career Grant MCB-0955407 awarded to E.C.Y.Y., and NSF grant CHE-0911520 awarded to V.S.B.

REFERENCES

- (1) Schnapf, J. L.; Baylor, D. A. *Sci. Am.* **1987**, *256*, 40.
- (2) Brown, P. K.; Wald, G. *Science* **1964**, *144*, 45.
- (3) Yau, K. W. *Invest. Ophthalmol. Visual Sci.* **1994**, *35*, 9.
- (4) Okada, T.; Ernst, O. P.; Palczewski, K.; Hofmann, K. P. *Trends Biochem. Sci.* **2001**, *26*, 318.
- (5) Wald, G. *Science* **1968**, *162*, 230.
- (6) Nathans, J. *Neuron* **1999**, *24*, 299.
- (7) Nathans, J.; Piantanida, T. P.; Eddy, R. L.; Shows, T. B.; Hogness, D. S. *Science* **1986**, *232*, 203.
- (8) Bok, D. *J. Cell Sci.* **1993**, 189.
- (9) Redmond, T. M.; Yu, S.; Lee, E.; Bok, D.; Hamasaki, D.; Chen, N.; Goletz, P.; Ma, J. X.; Crouch, R. K.; Pfeifer, K. *Nat. Genet.* **1998**, *20*, 344.
- (10) Yokoyama, S. *Prog. Retinal Eye Res.* **2000**, *19*, 385.
- (11) Bowmaker, J. K. *Vision Res.* **2008**, *48*, 2022.
- (12) Yokoyama, S. *Annu. Rev. Genomics Hum. Genet.* **2008**, *9*, 259.
- (13) Hunt, D. M.; Carvalho, L. S.; Cowing, J. A.; Davies, W. L. *Philos. Trans. R. Soc. B* **2009**, *364*, 2941.
- (14) Shichida, Y.; Matsuyama, T. *Philos. Trans. R. Soc. B* **2009**, *364*, 2881.
- (15) Yokoyama, S. *Annu. Rev. Genet.* **1997**, *31*, 315.
- (16) Sekharan, S.; Katayama, K.; Kandori, H.; Morokuma, K. *J. Am. Chem. Soc.* **2012**, *134*, 10706.
- (17) Rieke, F.; Baylor, D. A. *Biophys. J.* **1996**, *71*, 2553.
- (18) Holcman, D.; Korenbrot, J. I. *J. Gen. Physiol.* **2005**, *125*, 641.
- (19) Angueyra, J. M.; Rieke, F. *Nat. Neurosci.* **2013**, *16*, 1692.
- (20) Janz, J. M.; Farrens, D. L. *J. Biol. Chem.* **2004**, *279*, 55886.
- (21) Janz, J. M.; Farrens, D. L. *Vision Res.* **2003**, *43*, 2991.
- (22) Guo, Y.; Sekharan, S.; Liu, J.; Batista, V. S.; Tully, J. C.; Yan, E. C. Y. *Proc. Natl. Acad. Sci. U. S. A.* **2014**, *111*, 10438.
- (23) Vogel, R.; Siebert, F. *Biochemistry* **2002**, *41*, 3536.
- (24) Baylor, D. A.; Matthews, G.; Yau, K. W. *J. Physiol. (London, U. K.)* **1980**, *309*, 591.
- (25) Del Valle, L. J.; Ramon, E.; Bosch, L.; Manyosa, J.; Garriga, P. *Cell. Mol. Life Sci.* **2003**, *60*, 2532.
- (26) Liu, J.; Liu, M. Y.; Fu, L.; Zhu, G. A.; Yan, E. C. Y. *J. Biol. Chem.* **2011**, *286*, 38408.
- (27) Liu, M. Y.; Liu, J.; Mehrotra, D.; Liu, Y. T.; Guo, Y.; Baldera-Aguayo, P. A.; Mooney, V. L.; Nour, A. M.; Yan, E. C. Y. *J. Biol. Chem.* **2013**, *288*, 17698.
- (28) Liu, J.; Liu, M. Y.; Nguyen, J. B.; Bhagat, A.; Mooney, V.; Yan, E. C. Y. *J. Biol. Chem.* **2011**, *286*, 27622.
- (29) Liu, J.; Liu, M. Y.; Nguyen, J. B.; Bhagat, A.; Mooney, V.; Yan, E. C. Y. *J. Am. Chem. Soc.* **2009**, *131*, 8750.
- (30) Guo, Y.; Sekharan, S.; Liu, J.; Batista, V. S.; Tully, J. C.; Yan, E. C. Y. *Proc. Natl. Acad. Sci. U. S. A.* **2014**, *111*, 10438.
- (31) Sakmar, T. P.; Franke, R. R.; Khorana, H. G. *Proc. Natl. Acad. Sci. U. S. A.* **1989**, *86*, 8309.
- (32) Nickle, B.; Wilkie, S. E.; Cowing, J. A.; Hunt, D. M.; Robinson, P. R. *Biochemistry* **2006**, *45*, 7307.
- (33) Vought, B. W.; Dukkipati, A.; Max, M.; Knox, B. E.; Birge, R. R. *Biochemistry* **1999**, *38*, 11287.
- (34) Kono, M. *FEBS Lett.* **2006**, *580*, 229.

- (35) Tsutsui, K.; Imai, H.; Shichida, Y. *Biochemistry* **2007**, *46*, 6437.
- (36) Tsutsui, K.; Imai, H.; Shichida, Y. *Biochemistry* **2008**, *47*, 10829.
- (37) Sekharan, S.; Mooney, V. L.; Rivalta, I.; Kazmi, M. A.; Neitz, M.; Neitz, J.; Sakmar, T. P.; Yan, E. C.; Batista, V. S. *J. Am. Chem. Soc.* **2013**, *135*, 19064.
- (38) Yan, E. C. Y.; Epps, J.; Lewis, J. W.; Szundi, I.; Bhagat, A.; Sakmar, T. P.; Kliger, D. S. *J. Phys. Chem. C* **2007**, *111*, 8843.
- (39) Reeves, P. J.; Kim, J. M.; Khorana, H. G. *Proc. Natl. Acad. Sci. U. S. A.* **2002**, *99*, 13413.
- (40) Babu, K. R.; Dukkipati, A.; Birge, R. R.; Knox, B. E. *Biochemistry* **2001**, *40*, 13760.
- (41) Oprian, D. D.; Molday, R. S.; Kaufman, R. J.; Khorana, H. G. *Proc. Natl. Acad. Sci. U. S. A.* **1987**, *84*, 8874.
- (42) Chan, T.; Lee, M.; Sakmar, T. P. *J. Biol. Chem.* **1992**, *267*, 9478.
- (43) Franke, R. R.; Sakmar, T. P.; Graham, R. M.; Khorana, H. G. *J. Biol. Chem.* **1992**, *267*, 14767.
- (44) Fu, Y.; Kefalov, V.; Luo, D.-G.; Xue, T.; Yau, K.-W. *Nat. Neurosci.* **2008**, *11*, 565.
- (45) Rieke, F.; Baylor, D. A. *Neuron* **2000**, *26*, 181.
- (46) Sakurai, K.; Onishi, A.; Imai, H.; Chisaka, O.; Ueda, Y.; Usukura, J.; Nakatani, K.; Shichida, Y. *J. Gen. Physiol.* **2007**, *130*, 21.
- (47) Shichida, Y.; Imai, H.; Imamoto, Y.; Fukada, Y.; Yoshizawa, T. *Biochemistry* **1994**, *33*, 9040.
- (48) Imai, H.; Kuwayama, S.; Onishi, A.; Morizumi, T.; Chisaka, O.; Shichida, Y. *Photochem. Photobiol. Sci.* **2005**, *4*, 667.
- (49) Chen, M. H.; Kuemmel, C.; Birge, R. R.; Knox, B. E. *Biochemistry* **2012**, *51*, 4117.
- (50) Imamoto, Y.; Seki, I.; Yamashita, T.; Shichida, Y. *Biochemistry* **2013**, *52*, 3010.
- (51) Jastrzebska, B.; Palczewski, K.; Golczak, M. *J. Biol. Chem.* **2011**, *286*, 18930.
- (52) Lin, S. W.; Groesbeek, M.; van der Hoef, I.; Verdegem, P.; Lugtenburg, J.; Mathies, R. A. *J. Phys. Chem. B* **1998**, *102*, 2787.
- (53) Salgado, G. F. J.; Struts, A. V.; Tanaka, K.; Fujioka, N.; Nakanishi, K.; Brown, M. F. *Biochemistry* **2004**, *43*, 12819.
- (54) Kim, J. M.; Altenbach, C.; Kono, M.; Oprian, D. D.; Hubbell, W. L.; Khorana, H. G. *Proc. Natl. Acad. Sci. U. S. A.* **2004**, *101*, 12508.
- (55) Li, J.; Edwards, P. C.; Burghammer, M.; Villa, C.; Schertler, G. F. X. *J. Mol. Biol.* **2004**, *343*, 1409.
- (56) Palczewski, K.; Kumasaka, T.; Hori, T.; Behnke, C. A.; Motoshima, H.; Fox, B. A.; Le Trong, I.; Teller, D. C.; Okada, T.; Stenkamp, R. E.; Yamamoto, M.; Miyano, M. *Science* **2000**, *289*, 739.
- (57) Barlow, R. B.; Birge, R. R.; Kaplan, E.; Tallent, J. R. *Nature* **1993**, *366*, 64.
- (58) Mooney, V. L.; Szundi, I.; Lewis, J. W.; Yan, E. C.; Kliger, D. S. *Biochemistry* **2012**, *51*, 2630.
- (59) Yuan, S.; Filipek, S.; Palczewski, K.; Vogel, H. *Nat. Commun.* **2014**, *5*, 4733.